

Articles

Selectively Targeting T- and B-Cell Lymphomas: A Benzothiazole Antagonist of $\alpha_4\beta_1$ Integrin

Richard D. Carpenter,[†] Mirela Andrei,[‡] Olulanu H. Aina,[‡] Edmond Y. Lau,[§] Felice C. Lightstone,[§] Ruiwu Liu,[‡] Kit S. Lam,^{*,‡} and Mark J. Kurth^{*,†}

Department of Chemistry, University of California Davis, One Shields Avenue, Davis, California 95616, Department of Internal Medicine, Division of Hematology/Oncology, UC Davis Cancer Center, 4501 X Street, Sacramento, California 95817, Chemistry, Materials, Earth, and Life Sciences, Lawrence Livermore National Laboratory, 7000 East Street, Livermore, California 94550

Received March 19, 2008

Current cancer chemotherapeutic agents clinically deployed today are designed to be indiscriminately cytotoxic, however, achieving selective targeting of cancer malignancies would allow for improved diagnostic and chemotherapeutic tools. Integrin $\alpha_4\beta_1$, a heterodimeric cell surface receptor, is believed to have a low-affinity conformation in resting normal lymphocytes and an activated high-affinity conformation in cancerous cells, specifically T- and B-cell lymphomas. This highly attractive yet poorly understood receptor has been selectively targeted with the bisaryl urea peptidomimetic antagonist **1**. However, concerns regarding its preliminary pharmacokinetic (PK) profile provided an impetus to change the pharmacophore from a bisaryl urea to a 2-arylaminobenzothiazole moiety, resulting in an analogue with improved physicochemical properties, solubility, and kidney:tumor ratio while maintaining potency (**6**; IC₅₀ = 53 pM). The results presented herein utilized heterocyclic and solid-phase chemistry, cell adhesion assay, and in vivo optical imaging using the cyanine dye Cy5.5 conjugate.

Introduction

Many of the current cancer chemotherapeutic agents clinically deployed today are designed to be indiscriminately cytotoxic through DNA alkylation, unnatural base-pair incorporation, inhibition of topoisomerases, and microtubule stabilization mechanisms. Cancer chemotherapy, often administered near its maximum tolerated dose (MTD^a), aims to annihilate tumors with tolerable toxicity. Several of these agents exemplified in Figure 1 possess a narrow therapeutic index that limits effectiveness. As a consequence, underdosing at the tumor site is problematic, with patients suffering from significant side effects including nausea, vomiting, diarrhea, malnutrition, hair and memory loss, anemia, immunosuppression, hemorrhaging, chronic pain, and various organ toxicities. Tremendous success has been achieved

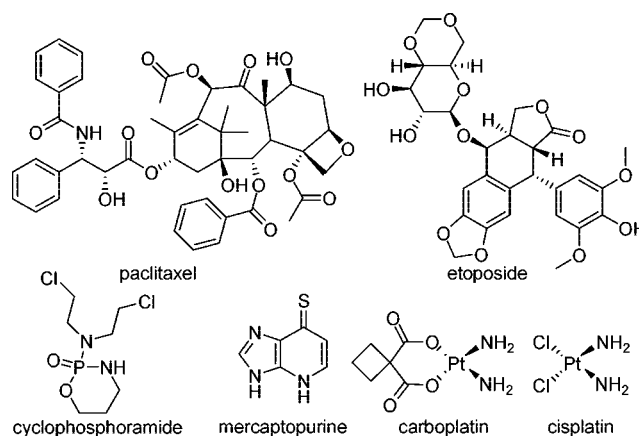


Figure 1. Structures of commonly administered indiscriminating cytotoxic chemotherapeutic agents.

through lengthy syntheses of ornate cytotoxic natural products with significantly less attention being granted toward *selective* chemotherapeutics that would result in decreased off-target binding and ensuing side effects.

To achieve target selectivity, therapeutic compounds must be able to differentiate cancer cells from normal cells. In T- and B-cell lymphomas, targeting the activated form of cell surface receptors expressed on cancer cells allows for differentiation, as normal or inactivated versions remain untargeted. Specifically, the cell surface receptor $\alpha_4\beta_1$ integrin regulates lymphocyte trafficking¹ and homing in normal adult cells.^{2,3} A β -subunit conformational change⁴ activates $\alpha_4\beta_1$, which regulates tumor growth, metastasis, and angiogenesis, in addition to promoting the dissemination of tumor cells to distal organs.⁵ The ligand LLP2A (**1**; see Figure 2) recognizes this change and shows potential as a noninvasive imaging and therapeutic agent

^a To whom correspondence should be addressed. For K.S.L.: phone, (916) 734-8012; fax, 916-734-7946; E-mail: kit.lam@ucdmc.ucdavis.edu. For M.J.K.: phone, (530) 752-8895; fax, 530-752-8895; E-mail: mjkurth@ucdavis.edu.

[†] Department of Chemistry, University of California Davis.

[‡] Department of Internal Medicine, Division of Hematology/Oncology, UC Davis Cancer Center.

[§] Chemistry, Materials, Earth, and Life Sciences, Lawrence Livermore National Laboratory.

^a Abbreviations: PK, pharmacokinetic; MTD, maximum tolerated dose; MIDAS, metal ion-dependent adhesion site; PEG, polyethylene glycol; FOS, function-oriented synthesis; Fmoc-Ach-OH, 1-[(9H-fluoren-9-yl)methoxy]carbonylamino]cyclohexanecarboxylic acid; HOBt, hydroxybenzotriazole; DIC, 1,3-diisopropylcarbodiimide; DMF, *N,N*-dimethylformamide; Fmoc-Aad(*t*Bu)-OH, (S)-2-[(9H-fluoren-9-yl)methoxy]carbonylamino]-6-*tert*-butoxy-6-oxohexanoic acid; DdeK(Fmoc)OH, (S)-6-[(9H-fluoren-9-yl)methoxy]carbonylamino]-2-[1-(4,4-dimethyl-2,6-dioxocyclohexylidene)ethylamino]hexanoic acid; HBTU, 2-(1*H*-benzotriazol-1-yl)-1,1,3,3-tetramethyluronium hexafluorophosphate; DIEA, diisopropylethylamine; TFA, trifluoroacetic acid; BSA, bovine serum albumin; PBS, phosphate-buffered saline; FmocK(Dde)OH, (S)-2-[(9H-fluoren-9-yl)methoxy]carbonylamino]-6-[1-(4,4-dimethyl-2,6-dioxocyclohexylidene)ethylamino]hexanoic acid; FmocK-(Alloc)OH, (S)-1-(9H-fluoren-9-yl)-3,11-dioxo-2,12-dioxo-4,10-diazapentadec-14-ene-5-carboxylic acid.

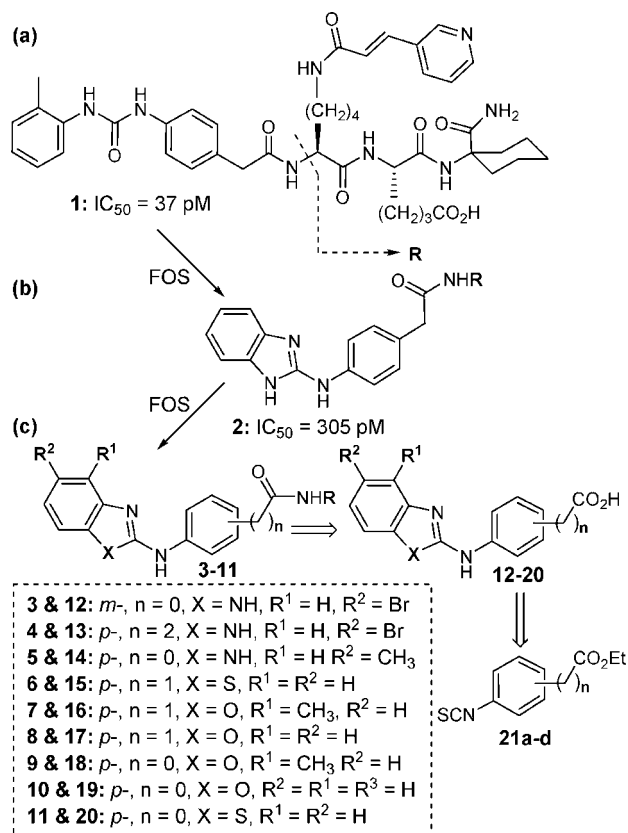


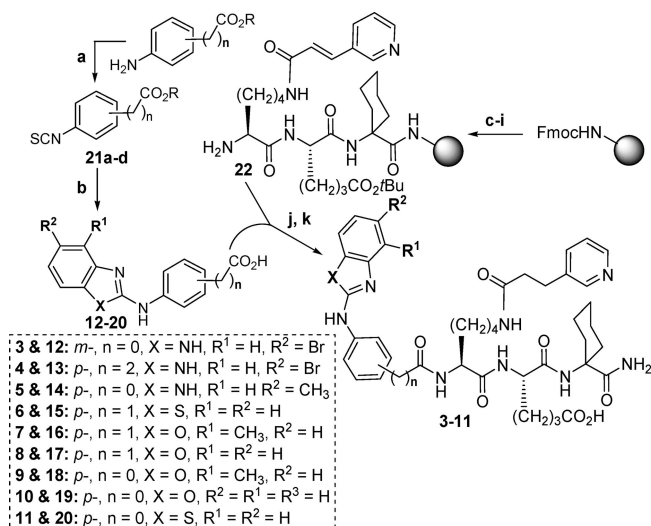
Figure 2. Evolution of ligand analogues using function-oriented synthesis (FOS): (a) Structure of **1** (LLP2A), which can be optically or radioconjugated and shows potential as an imaging or therapeutic agent for lymphoma;⁶ (b) structure of water soluble benzimidazole analogue **2** (IC₅₀ = 305 pM);⁷ (c) heterocyclic analogues **3–11** and requisite precursor heterocyclic acids **12–21** and aryl isothiocyanates **21a–d**.

despite kidney uptake observed in xenograft models.⁶ This prompted creation of a water soluble benzimidazole analogue KLCA4 (**2**)⁷ that would be dianionic⁸ at physiological pH (bisarylamino NH + CO₂H), thereby improving solubility and decreasing kidney uptake based on electronic factors.^{7,9,10} While **2** has picomolar potency, it is still 10-fold less potent than the bisaryl urea **1**. Herein, we report the design of an equipotent (to **1**), comparably soluble (to **2**) benzothiazole analogue **6** that, when optically conjugated using Cy5.5, demonstrates excellent tumor uptake with preliminary evidence showing an improved kidney:tumor ratio in xenograft models. Key to this approach is the heterocyclic design, which, in a condensed fashion, improves the ligand's physicochemical properties without PEGylation or a poly charged tail.

Results and Discussion

Our previous benzimidazole ligand showed excellent binding to human $\alpha_4\beta_1$ integrin; however, it still did not bind as efficiently as LLP2A (**1**). The design of improved analogues, was centered around systematic modifications to the heterocycle, its substituents, and its side chain to regain the binding affinity while improving the pharmacokinetics over previous leads. As delineated in Scheme 1, *m*- and *p*-aniline esters were thiophosgenated, delivering the aryl isothiocyanate esters **21a–d** in 81–93% yield. These aryl isothiocyanate esters were then reacted with 4,5-diversified *o*-nucleophilic anilines, yielding thiourea intermediates that undergo a tandem reaction with a carbodiimide-resin to deliver thiocondensed heterocyclic esters.

Scheme 1. Synthesis of Analogues **3–11** (See Supporting Information for Structures)^a



^a (a) (Cl)₂C=S, Et₃N, EtOAc; (b) 5-*R*²-4-*R*³-2-XH-anilines, CH₂Cl₂, 16 h, followed by *N*-cyclohexylcarbodiimide, *N*'-methyl polystyrene resin, then LiOH, H₂O/dioxane, Δ; (c) swell/DMF, 3 h; (d) 20% piperidine/DMF; (e) Fmoc-Ach-OH, DIC, HOBT, DMF; → (d); (f) Fmoc-Aad(*t*Bu)-OH, DIC, HOBT, DMF; → (d); (g) Dde-K(Fmoc)-OH, DIC, HOBT, DMF; → (d); (h) (*E*)-3-(pyridin-3-yl)acrylic acid, DIC, HOBT, DMF; (i) 2% H₂NNH₂/DMF; (j) **12–20**, HBTU, EtN(*i*Pr)₂, DMF; (k) TFA, (*i*Pr)₃SiH, H₂O.

The removal of the polystyrene-bound thiourea by filtration simplifies purification and this technology allows for the extension of a previously reported benzimidazole preparation¹¹ to benzoxazole and benzothiazole systems as well. The resulting heterocyclic esters, when subjected to saponification conditions, deliver the *m*- and *p*-heterocyclic acid precursors **12–20** in 68–84% overall yield from the aryl isothiocyanate. Diversification at the *o*-position was precluded due to a 6-*exo*-trig cyclization under saponification conditions affording benzimidazoquinazolinones.¹²

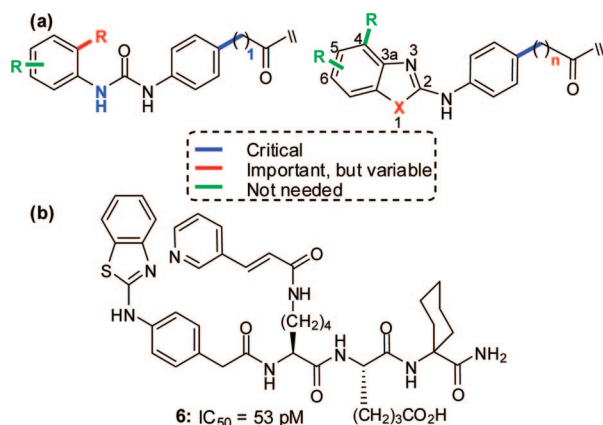
Effort was next forwarded on preparing the Rink resin-bound tripeptide **22** and analogue targets **3–11**. Tripeptide **22** was prepared by first Fmoc-deprotecting Rink resin followed by activating an appropriately protected amino acid via treatment with DIC/HOBT in DMF and addition of this solution to the resulting amino resin. This process was repeated twice more with the respective precursors **12–20**, each dissolved in a solution of HBTU/DIEA and DMF, were coupled to the polymer-tripeptide **22**. No detectable polymerization occurred with the 2-arylaminoheterocyclic acids **12–20**, enabling this reaction to occur without additional protecting groups. The heterocyclic tripeptides were cleaved from the polymer under acidic conditions to give heterocyclic analogues **3–11** (see Table 1 for yields).

The potencies of these heterocyclic analogues were determined using a Molt-4 cell adhesion assay by inhibiting $\alpha_4\beta_1$ -mediated cell adhesion to the known ligand CS-1. A neutravidin-coated 96-well plate was incubated with biotinylated CS-1. The wells were then blocked, followed by incubation with Molt-4 cells expressing activated $\alpha_4\beta_1$ integrin (1.3×10^5 cells/well). Serially diluted ligands were incubated and washed; the remaining bound cells were then fixed and stained. Inhibition was quantified by measuring absorbance at 570 nm and IC₅₀ data were extrapolated from the concentration-dependent inhibition curves.

The SAR data for this class of compounds is summarized in Table 1 and Figure 3, with *p*-orientation being critical as

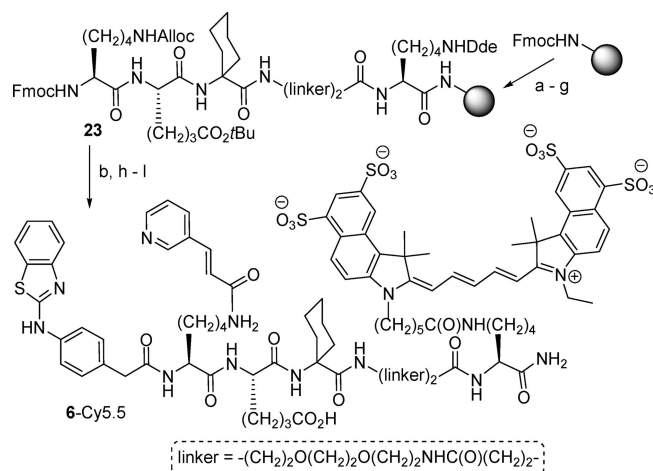
Table 1. Overall Yield, Purity, Molecular Ion, and IC₅₀ of Heterocyclic Analogues

compound	yield, %	purity, %	[M + H] ⁺	IC ₅₀
1				37 pM
2				305 pM
3	50	97	858, 860	30 nM
4	54	98	886, 888	379 nM
5	44	95	794	490 nM
6	62	100	811	53 pM
7	74	99	809	4 nM
8	69	100	794	2 nM
9	61	99	795	1 μM
10	64	100	781	1 μM
11	58	100	797	347 nM

**Figure 3.** (a) Original SAR findings of **1** juxtaposed to that of the heterocyclic analogues. (b) Structure of the equipotent (to **1**) benzothiazole acetamide **6**.

m-substitution was impotent. Moreover, carboxamides (where $n = 0$) were largely ineffective in achieving an equipotent analogue. The benzoxazole **9** and 4-methylbenzoxazole **10** showed complete loss of potency, while benzothiazole **11**, and 5⁶-methylbenzimidazole **5** showed mid nM potency. The 4-methylbenzoxazole acetamide **7** exhibited low nM potency. While holding constant the acetamide ($n = 1$), removal of the methyl group results in no appreciable change for benzoxazole **8**, but replacement of $X = O$, NH with $X = S$ in benzothiazole **6** further increases the potency to the low pM range (IC₅₀ = 53 pM). From nine heterocyclic analogues, the benzothiazole acetamide **6** was discovered to be equipotent to **1**. The sulfur atom is probably an isostere for the NH moiety of **2** as both heteroaryl rings are likely antiperiplanar to the phenyl ring. The benzoxazole **8**, however, adopts a near-planar orientation likely making the smaller oxygen atom a less successful isostere.

Near-infrared optical imaging preliminary studies were then performed to measure tumor and organ uptake in lymphoma xenograft bearing murine models using the fluorophore Cy5.5-labeled benzothiazole acetamide. While this conjugate is not ideal in terms of size and sophistication (triples the molecular weight; 5-fold cost increase), this allows for safe, nonradioactive studies to initially assess in vivo biological activity before radio studies. Scheme 2 delineates the synthesis of **6-Cy5.5** starting with Rink amide resin, followed by a series of Fmoc-deprotection and *N*-acylation iterations with appropriately protected amino acids and linkers delivering resin **23**. Key to this synthesis is the use of two orthogonally protected lysines that will be selectively deprotected as well as a hydrophilic linker to minimize dye interference with integrin binding. The α -carbamate of lysine was Fmoc-deprotected and *N*-acylated with the benzothiazole phenylacetic acid **15** under HBTU/DIEA conditions. Chemoselective deprotection of the Alloc group with

Scheme 2^a

^a Reagents and conditions: (a) swell, DMF, 24 h; (b) 20% piperidine/DMF; (c) Fmoc-K(Dde)-OH, DIC, HOBT, DMF → (b); (d) Fmoc-NH-linker-CO₂H, DIC, HOBT, DMF → (b) → (d) → (b); (e) Fmoc-Ach-OH, DIC, HOBT, DMF → (b); (f) Fmoc-Aad(OtBu)-OH, DIC, HOBT, DMF → (b); (g) Fmoc-K(Alloc)-OH, DIC, HOBT, DMF → (b); (h) (i) **15**, HBTU, DIEA, DMF; (ii) Pd(PPh₃)₄, PhSiH₃, DMF; (i) (*E*)-3-(pyridin-3-yl)acrylic acid, DIC, HOBT, DMF; (j) 2% H₂NNH₂/DMF; (k) Cy5.5-NHS, DIEA, DMF; (l) TFA, H₂O, (*i*Pr)₃SiH.

Pd⁰ and phenylsilane (**Caution**: Pressure buildup!) followed by *N*-acylation of the resulting amine with 3-pyridylacrylic acid affords an intermediate with the complete framework of **6**. Deprotection of the Dde group, *N*-acylation with Cy5.5-NHS, and acid hydrolysis liberates **6-Cy5.5** from the solid support with concomitant deprotection of the *t*-butyl ester.

Keeping in mind that a safe in vivo evaluation was desired prior to radio studies, activated $\alpha_4\beta_1$ expressed Molt-4 (T-cell lymphoma) or Raji tumors (B-cell lymphoma) were subcutaneously implanted into the right shoulder of the nude mice. As a negative control, A549 nonsmall cell lung cancer (not expressing $\alpha_4\beta_1$) was implanted into the left shoulder. To establish adequate doses, varying amounts of **6-Cy5.5** were administered via the tail vein into nude mice bearing subcutaneously Molt-4 or Raji and A549 xenografts. As depicted in Figure 4, some mice were serially imaged ranging from 5 min to 120 h post injection. Other mice were sacrificed at various time points, with ex vivo specificity and uptake measurements of pertinent organs and tumors for both agents at similar doses. Tumor uptake was observed as early as 5 min post injection and persisted for up to 120 h. To determine organ:tumor ratios, regions of interest were drawn around the tumor and each organ in the ex vivo images and mean signal intensity was obtained by subtracting the lowest intensity background signal (heart) from each intensity value. Preliminary evidence indicates **6-Cy5.5** is comparable to **1-Cy5.5** in terms of tumor specificity and uptake while showing improvement in the kidney:tumor ratio. Regardless of the imaging agent, an appropriate decrease in signal is observed as the dose decreases. Furthermore, both agents showed low liver, muscle, lung, and spleen signal while consistently showing skin, lymph node, and negative tumor signal. Optical probe uptake by the $\alpha_4\beta_1$ integrin negative tumors may in part be explained by the expression of activated $\alpha_4\beta_1$ integrin in tumor vasculature.¹³ These findings strengthen the hypothesis that the improved kidney:tumor ratio may be attributed to the presence of an additional negative charge from the arylaminobenzothiazole N-H⁸ at physiological pH. This

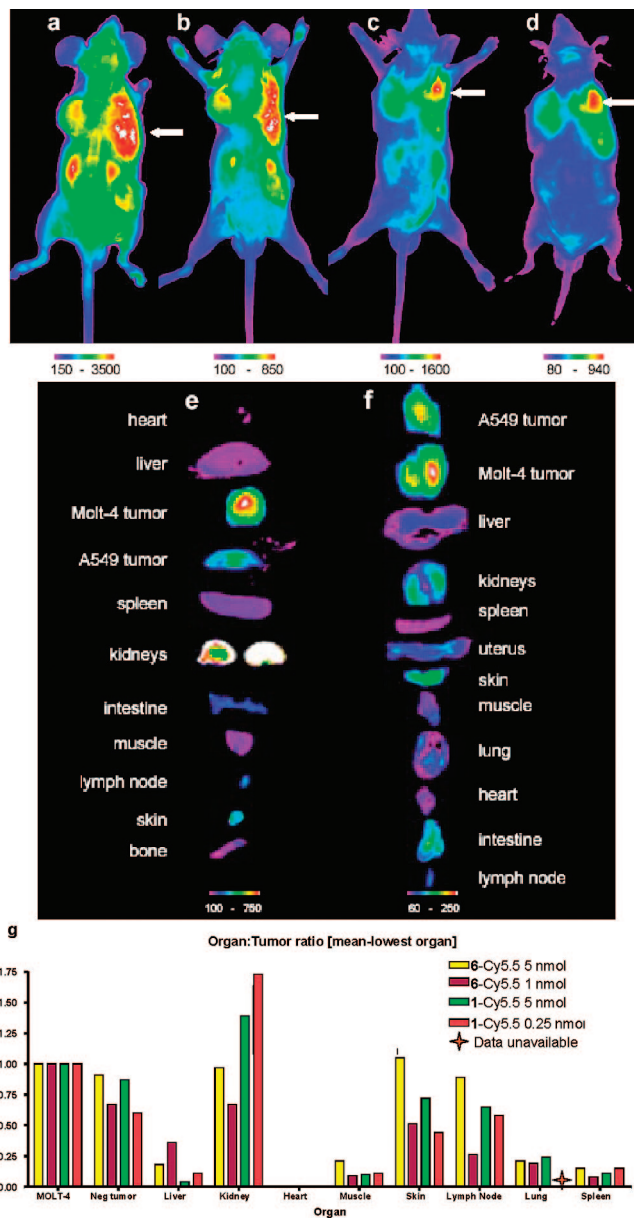


Figure 4. In vivo near-infrared light (NIRF) images using 100 μL of 6-Cy5.5 with $\alpha_4\beta_1$ -bearing tumors grown on the upper right side (Molt-4), lower right side (Raji), and non- $\alpha_4\beta_1$ -bearing tumor grown on the left side as a negative control (A549) at the following doses and times: (a) 10 nmol, $t = 4$ h; (b) 10 nmol, $t = 24$ h; (c) 10 nmol, $t = 48$ h; (d) 10 nmol, $t = 120$ h. Ex vivo NIRF image mean intensity values 24 h postinjection of pertinent organs and tumors at the following doses: (e) 1-Cy5.5 (0.25 nmol, 24 h postinjection); and (f) 6-Cy5.5 (1 nmol, 24 h postinjection). Ex vivo NIRF image graphs (g) Side-by-side organ: tumor [mean-lowest organ] ratio at comparable doses for 1-Cy5.5 and 6-Cy5.5. Note that lung images were not available for 0.25 nmol 1-Cy5.5.

additional negative charge aids in solubility and may promote excretion by preventing kidney uptake.

Conclusion

Using synthesis, cell adhesion assays, and optical imaging with xenograft murine models, the bisaryl urea moiety (**1**) has been transformed from a bisaryl urea to the benzothiazole analogue **6** without sacrificing low picomolar potency to activated $\alpha_4\beta_1$ integrin. Because of the presence of an additional acidic hydrogen from a relatively unusual acid (bisarylamino

NH), preliminary evidence shows the 6-Cy5.5 conjugate has improved solubility and kidney:tumor ratio while retaining excellent tumor uptake and comparable organ specificity. This work further enables lymphoma targeting with a highly potent ligand and highlights the importance of physicochemical factors in the rational design of analogues to maintain potency while preventing toxicity. Although 6-Cy5.5 is not an ideal agent, these nonradioactive preliminary in vivo optical studies show encouraging results, with future efforts pointing toward the incorporation of radioisotopes for more rigorous pharmacokinetic and radio chemotherapeutic and/or imaging purposes.

Experimental Section

General Synthetic Procedures. All chemicals were purchased from commercial suppliers and used without further purification. Rink amide resin (0.5 mmol/g loading, 100–200 mesh) was purchased from Tianjin Nankai Hecheng Sci & Tech. Co., Ltd., (batch number GRM-0406-J). *N*-cyclohexylcarbodiimide, *N*'-methyl polystyrene resin (1.3 mmol/g loading, 200–400 mesh) was purchased from Novabiochem. Analytical TLC was carried out on precoated plates (silica gel 60, F254) and visualized with UV light. NMR spectra (^1H at 300 MHz, 400 MHz, 600 MHz; ^{13}C at 75 MHz, 100 MHz) were recorded in $\text{DMSO-}d_6$, methanol- d_4 , and acetone- d_6 as solvents and chemical shifts are expressed in parts per million relative to residual undeuterated solvent. The specifications of the LC/MS are as follows: electrospray (+) ionization, mass range 100–900 Da, 20 V cone voltage, and Xterra MS C_{18} column (2.1 mm \times 50 mm \times 3.5 μm). CC refers to normal-phase silica-gel column chromatography. Concentration refers to rotary evaporation under reduced pressure. After each solid-phase step, the resin was washed by sequential treatment with the following solvents: DMF (2 \times 5 mL), H_2O (2 \times 5 mL), CH_3OH , (3 \times 5 mL), and CH_2Cl_2 (5 \times 5 mL).

General Procedure for Heterocyclic Acids: 4-(5⁶-Methyl-1H-benzod[*h*]imidazol-2-ylamino)benzoic Acid (14**).** Following our previously reported procedure,⁷ to a solution of *o*-phenylenediamine (1.90 g, 17.6 mmol) in CH_2Cl_2 (75 mL) was added a solution of the aryl isothiocyanate ester (For **2a**, 3.0 g, 16.8 mmol) in CH_2Cl_2 (75 mL) dropwise over 30 min, followed by stirring for 16 h at room temperature. After TLC showed that the aryl isothiocyanate was consumed, polystyrene-bound DCC resin was added [for **14**, (39 mg, 50.4 mmol)] and the reaction proceeded at room temperature until TLC showed the intermediate thiourea was consumed. In most instances, this was between 4–8 h, but in some cases this took as long as 16 h (**14**, 4.5 h). The resin was filtered, followed by concentration of the filtrate. The resulting residue was taken up in ethyl acetate/ H_2O , followed by washing (H_2O , brine), drying (MgSO_4), and concentrated to give the benzimidazole ester (4.08 g) that was used without further purification. A solution of this benzimidazole ester (4.08 g, 15.3 mmol) in dioxane/ H_2O (125 mL/80 mL) was treated with LiOH (1.83 g, 76.4 mmol) and the solution was refluxed for 16 h. The reaction mixture was concentrated, and the residue was taken up in aqueous 2 M NaOH. This basic water layer (pH \sim 10) was washed twice with ether before being acidified with concentrated HCl to pH \sim 2–3, at which point **14** precipitated as a light-gray solid (3.43 g, 74%): mp 368–370 $^\circ\text{C}$. IR (neat) 3542 (st, br), 3284 (sh), 3050 (sh), 2984, 1699 (st). ^1H (300 MHz, $\text{DMSO-}d_6$): δ 7.97 (d, $J = 6.6$ Hz, 2H), 7.58 (d, $J = 7.2$ Hz, 2H), 7.35 (d, $J = 7.8$ Hz, 1H), 7.28 (s, 1H), 7.05 (d, $J = 8.1$ Hz), 2.35 (s, 3H). ^{13}C NMR (75 MHz, $\text{DMSO-}d_6$): δ 166.9, 146.6, 141.3, 133.1, 131.1, 130.6, 128.4, 126.6, 124.6, 120.1, 112.3, 112.1, 21.2. ESI MS (m/z) 268 ($\text{M} + \text{H}$)⁺. Anal. Calcd for $\text{C}_{15}\text{H}_{13}\text{N}_3\text{O}$: C, 67.40; H, 4.90; N, 15.72. Found: C, 67.63; H, 4.91; N, 15.78. Purity was determined to be 99% by HPLC analysis on the basis of absorption at 220 nm.

$\text{H}_2\text{N-K}[(E)\text{-3-(Pyridin-3-yl)acrylamide}]\text{-Aad(O}t\text{Bu)-Ach-Rink Polystyrene (22)$. Rink amide resin (2.35 g, 1.19 mmol) was swollen in DMF (30 mL) for 3 h, followed by treatment with 20% piperidine in DMF (20 mL). After washing, the resin was then treated with a

premixed solution of Fmoc-Ach-OH (Fmoc-Ach-OH; 1.30 g, 3.57 mmol), 1,3-diisopropylcarbodiimide (DIC; 3.57 mmol, 553 μL), and hydroxybenzotriazole (HOBt; 482 mg, 3.57 mmol) in DMF (20 mL) followed by shaking for 6 h. After a negative Kaiser test¹⁴ washing, this sequence of deprotection/coupling was repeated thrice more with Fmoc-Aad(*t*Bu)-OH (Fmoc-Aad(*t*Bu)-OH; 1.57 g, 3.57 mmol), Dde-K(Fmoc)-OH (Dde-K(Fmoc)-OH; 1.85 g, 3.57 mmol), and (*E*)-3-(pyridin-3-yl)acrylic acid (532 mg, 3.57 mmol). After washing, the Dde-tripeptide resin was washed and treated with 2% H_2NNH_2 in DMF (20 mL) for 20 min, followed by washing to afford the free amino-tripeptide resin **22**: IR (neat) 3430 (sh), 3370 (sh), 3084, 1740 (st), 1684 (st), 1680 (st), 1662 (st), 1654 (st) cm^{-1} .

General Procedures for Heterocyclic Analogues: (R)-5-(R)-[2-(2-[4-(Benzothiazol-2-ylamino)-phenyl]acetylamin)-6-(E)-3-pyridin-3-yl-acryloylamino]hexanoylamino]-5-(1-carbamoylcyclohexylcarbamoyl)pentanoic Acid (6). Heterocyclic acid **15** (53 mg, 0.180 mmol), 2-(1*H*-benzotriazole-1-yl)-1,1,3,3-tetramethyluronium hexafluorophosphate (HBTU; 67 mg, 0.180 mmol), and DIEA (54.7 mL, 0.360 mmol) were dissolved in DMF (3 mL) and the homogeneous solution was allowed to stand for 10 min. This solution was then added to the free amino tripeptide resin **22** (120 mg, 0.06 mmol) and was shaken for 4 h. After washing, the resin was then cleaved with 3 mL of a 95:2.5:2.5 cleavage solution of TFA:H₂O:TIPS for 2 h, followed by draining and washing with the cleavage solution. This cleavage process was repeated once more, and the combined filtrates were concentrated under a gentle stream of nitrogen, precipitated with ether, centrifuged, and decanted. The precipitate was then purified by preparatory HPLC, and the combined fractions were lyophilized to afford **6** (27 mg, 62% from Rink Amide resin) as a white powder: ESI MS (*m/z*) 810 ($\text{M} + \text{H}$)⁺. EI HRMS (*m/z*) for C₄₂H₅₀N₈O₇S: Calcd 810.3523 ($\text{M} + \text{H}$)⁺. Found: 811.3549. Purity was determined to be 99% by HPLC analysis. Tabulated analytical data for **3–11** as well as **6-Cy5.5** are shown in Table 1 of the Supporting Information.

2-(1E,3E,5E)-5-3-(R)-1-(1-(R)-2-(R)-2-[2-(4-(Benzo[d]thiazol-2-ylamino)phenyl)acetamido]-6-(E)-3-(pyridin-3-yl)acrylamido)hexanamido)-5-carboxypentanamido)cyclohexyl)-27-carbamoyl-1,9,13,21,25,33-hexa-oxo-5,17-dioxo-2,8,14,20,26,32-hexa-azaheptatriacontan-37-yl)-1,1-dimethyl-6,8-disulfonato-1*H*-benzo[e]indol-2(3*H*)-ylid-ene)penta-1,3-dienyl)-3-ethyl-1,1-dimethyl-1*H*-ben-zo[e]indolium-6,8-disulfonate (6-Cy5.5). Rink amide resin (120 mg, 0.06 mmol) was swollen in DMF (3 mL) for 3 h, followed by treatment with 20% piperidine in DMF (20 mL). After washing, the resin was then treated with a premixed solution of Fmoc-K(Dde)-OH (93 mg, 0.180 mmol), 1,3-diisopropylcarbodiimide (DIC; 0.180 mmol, 27.9 μL), and hydroxybenzotriazole (HOBt; 24.3 mg, 0.180 mmol) in DMF (3 mL), followed by shaking for 6 h. After a negative Kaiser test¹⁴ washing, this sequence of deprotection/coupling was repeated with *N*-(Fmoc-8-amino-3,6-dioxo-octyl)succinamic acid (85 mg, 0.180 mmol), then Fmoc-Ach-OH (66 mg, 0.180 mmol), Fmoc-Aad(*O**t*Bu)-OH (79 mg, 0.180 mmol), and Fmoc-K(Alloc)-OH (82 mg, 0.180 mmol). The free α -amino resin was then treated with a premixed solution of **15** (51 mg, 0.180 mmol), HBTU (68 mg, 0.180 mmol), and DIEA (35.8 μL , 0.180 mmol) in DMF (3 mL) for 4 h. After washing, the ϵ -Alloc protected amine was deprotected by treatment with a solution of Pd(PPh₃)₄ (11 mg, 9 \times 10⁻³ mmol) and phenylsilane (1.2 mmol, 149 μL) in DMF (3 mL) for 30 min. **Note:** Care should be taken (*i.e.*, venting), as this reaction builds up heat and pressure. After draining and washing, this deprotection was repeated once more. This free ϵ -amino resin was then treated with a solution of (*E*)-3-(pyridin-3-yl)acrylic acid (27 mg, 0.180 mmol), DIC (0.180 mmol, 27.9 μL), and hydroxybenzotriazole (HOBt; 24.3 mg, 0.180 mmol) in DMF (3 mL). The ϵ -Dde protected amine was removed upon treatment with 2% H_2NNH_2 in DMF (3 mL) for 5 min, then washed with DMF and repeated for 15 min. After washing, to this free ϵ -amino resin was added Cy5.5-NHS (90 mg, 0.090 mmol) and DIEA (0.090 mmol, 15.8 μL) in DMF (3 mL) and allowed to shake for 8 h. After washing, the resin was then cleaved with 3 mL of a 95:2.5:2.5 cleavage solution of TFA:H₂O:TIPS for 2 h, followed by draining and washing with the cleavage solution. This cleavage

process was repeated once more, and the combined filtrates were concentrated under a gentle stream of nitrogen, precipitated with ether, centrifuged, and decanted. The precipitate was then purified by preparatory HPLC, and the combined fractions were lyophilized to afford **6-Cy5.5** (13 mg, 34%) as a blue powder: ESI MS (*m/z*) 2221 ($\text{M} + \text{H}$)⁺. ESI HRMS (*m/z*) for C₁₀₆H₁₃₁N₁₆NaO₂₃S₅: Calcd 2242.7882 ($\text{M} + \text{Na}$)⁺. Found: 2242.7871. Purity was determined to be 100% by HPLC analysis.

General Procedure for Aryl Isothiocyanate Esters: Ethyl 4-Isothiocyanatobenzoate (21a). Following our previously reported procedure,²¹ a solution of an appropriate aniline ester (4.5 g, 27.3 mmol) and triethylamine (60.1 mmol, 8.37 mL) in ethyl acetate (160 mL) was treated with thiophosgene (30.0 mmol, 2.30 mL) in ethyl acetate (130 mL) dropwise over 30 min at 0 °C. After addition, the cooling bath was removed and the reaction mixture was allowed to gradually warm up to room temperature over 12 h. The workup consisted of diluting with ethyl acetate, followed by washing sequentially with water (200 mL \times 2) and brine (200 mL). The organic layer was dried (MgSO₄), concentrated, and the crude product was purified via short path CC (hexanes/ethyl acetate, 9:1) to give **2a** (5.03 g, 89%). The analytical data are in accord with literature values.¹⁵

Ethyl 2-(4-Isothiocyanatophenyl)acetate (21b). Following the general procedure for aryl isothiocyanate esters yielded **2b** (5.20 g, 93%). The analytical data are in accord with literature values.¹⁶

Methyl 3-(4-Isothiocyanatophenyl)propanoate (21c). Following the general procedure for aryl isothiocyanate esters yielded **21c** (5.41 g, 90%). The analytical data are in accord with literature values.^{7,17}

Methyl 3-Isothiocyanatobenzoate (21d). Following the general procedure for aryl isothiocyanate esters yielded **21d** (7.06 g, 92% yield). The analytical data are in accord with literature values.¹⁸

3-(5⁶-Bromo-1*H*-benzo[d]imidazol-2-ylamino)benzoic Acid (12). Following the general procedure for heterocyclic acids yielded **12** (Yield 1.27 g, 78%). The analytical data are in accord with our previously reported values.⁷

3-(4-(5⁶-Bromo-1*H*-benzo[d]imidazol-2-ylamino)phenyl)propanoic Acid (13). Following the general procedure for heterocyclic acids yielded **13** (Yield 1.82 g, 83%). The analytical data are in accord with our previously reported values.⁷

2-(4-(Benzo[d]thiazol-2-ylamino)phenyl)acetic Acid (15). Following the general procedure for heterocyclic acids yielded **15** (2.81 g, 70%). The analytical data are in accord with literature values.¹⁹

2-(4-(4-Methylbenzo[d]oxazol-2-ylamino)phenyl)acetic Acid (16). Following the general procedure for heterocyclic acids yielded **16** (2.49 g, 75%) as a gray solid: mp 337–339 °C. IR (neat) 3539 (st, br), 3268 (sh), 3049 (sh), 2984, 1724 (st). ¹H (400 MHz, DMSO-*d*₆): δ 10.56 (br s, 1H), 7.69 (d, *J* = 6.8 Hz, 2H), 7.24 (apparent t, 3H), 7.02–6.95 (m, 2H), 3.50 (s, 2H), 2.47 (s, 3H). ¹³C NMR (100 MHz, DMSO-*d*₆): δ 172.9, 157.5, 146.6, 141.3, 137.5, 129.9, 128.6, 126.3, 124.7, 121.3, 117.5, 106.4, 22.5, 16.2. ESI MS (*m/z*) 283 ($\text{M} + \text{H}$)⁺. Anal. Calcd for C₁₆H₁₄N₂O₃: C, 68.07; H, 5.00; N, 9.92. Found: C, 68.18; H, 5.00; N, 9.95. Purity was determined to be 99% by HPLC analysis on the basis of absorption at 220 nm.

2-(4-(Benzo[d]oxazol-2-ylamino)phenyl)acetic Acid (17). Following the general procedure for heterocyclic acids yielded **17** (1.89 g, 79%). The analytical data are in accord with literature values.²⁰

4-(4-Methylbenzo[d]oxazol-2-ylamino)benzoic Acid (18). Following the general procedure for heterocyclic acids yielded **18** (1.67 g, 81%) as a light tan solid: mp 327–329 °C. IR (neat) 3560 (st, br), 3248 (sh), 3032 (sh), 2994, 1696 (st). ¹H (300 MHz, DMSO-*d*₆): δ 11.11 (s, 1H), 7.96 (d, *J* = 9 Hz, 2H), 7.91 (d, *J* = 9 Hz, 2H), 7.26 (apparent t, 1H), 7.01–6.97 (m, 2H), 2.45 (s, 3H). ¹³C NMR (75 MHz, DMSO-*d*₆): δ 167.2, 156.9, 146.7, 143.1, 141.0, 130.8, 126.8, 124.8, 123.9, 121.9, 116.8, 106.6, 16.3. ESI MS (*m/z*) 269 ($\text{M} + \text{H}$)⁺. Anal. Calcd for C₁₅H₁₂N₂O₃: C, 67.16; H, 4.51; N, 10.44. Found: C, 66.93; H, 5.34; N, 10.09. Purity was determined to be 99% by HPLC analysis on the basis of absorption at 220 nm.

4-(Benzo[d]oxazol-2-ylamino)benzoic Acid (19). Following the general procedure for heterocyclic acids yielded **19** (2.04 g, 76%). The analytical data are in accord with literature values.²¹

4-(Benzo[d]thiazol-2-ylamino)benzoic Acid (20). Following the general procedure for heterocyclic acids yielded **20** (1.19 g, 85%). The analytical data are in accord with literature values.²²

Cell Adhesion Assay Background. $\alpha_4\beta_1$ integrins are cell surface heterodimeric glycoproteins that mediate cell adhesion to vascular cell adhesion molecule-1 (VCAM-1 or CD 106) as well as to extracellular matrix (ECM) protein fibronectin (FN).⁴ Integrin expression and function depend on cell activation. The dynamic changes in integrin affinity, avidity, or activation state are implicated in cell migration, survival and apoptosis, cancer development, and metastasis.²³ Binding affinities (IC50s) of the ligands were studied in a Molt4 T-cell leukemia adhesion assay by inhibiting the $\alpha_4\beta_1$ -mediated cell adhesion to CS-1 peptide (DELPQLVTLPHPNLHGPEILDVPST), which is the binding motif of fibronectin to $\alpha_4\beta_1$ receptor.

General Procedure for Cell Adhesion Assay. We prepared 96-well plates by coating them with 1 $\mu\text{g/mL}$ neutravidin for a one-hour period, followed by adding 2 μM biotin-conjugated CS-1 peptide. The wells were then blocked with 1% bovine serum albumin in phosphate buffer saline (PBS) solution, followed by adding a volume of 80 μL consisted of 1.3×10^5 Molt4 cells, and finally different dilutions of tested ligands in binding buffer (1 mM Mn^{2+} TBS) were added to each well. To allow binding, the plates were incubated for 30 min at 37 °C, followed by washing of unbound cells with PBS. Bound cells were fixed with 10% formalin buffered in phosphate for 30 min and stained with 0.1% crystal violet. After washing and drying at room temperature, the dye was dissolved in 1% SDS, and absorbance at 570 nm was measured using a 96-well TECAN OD UV/vis spectrophotometer. Inhibition was calculated as a percentage resulting from the concentration-dependent curve.

Xenograft Methods. Four–six week old male and female athymic nude (Nu/Nu) mice were purchased from Harlan Sprague–Dawley (Indianapolis, IN). Mice were housed in the animal facility and fed ad lib with rodent pellets and water. Tumor xenografts were created by injecting Molt-4 (T-cell lymphoma) or Raji (B-cell lymphoma; 1×10^7 cells in 200 μL incomplete RPMI media) subcutaneously on the right upper back and A549 (1×10^6 cells in 200 μL incomplete DMEM media) subcutaneously on the left upper back under mild inhalation anesthesia (halothane). Studies commenced when xenografts reached between 10–15 mm. All procedures were conducted under an approved protocol according to guidelines specified by the National Institute of Health Guide for Animal Use and Care. Animals were anesthetized intraperitoneally with (1 $\mu\text{L/g}$ bwt) of 6 mg/mL pentobarbital sodium. The tails were dilated with warm water and animal were injected iv. Animals were imaged serially for tumor uptake and washout. The duration of each scan was 30 s for each acquired exposure.

Acknowledgment. This research is dedicated to the legacy of Dorothy Schoening who lost her lymphoma battle December 4, 2005. R.D.C. thanks the American Chemical Society's Division of Medicinal Chemistry for their Predoctoral Fellowship, the Howard Hughes Medical Institute for their Med into Grad Fellowship, and UC Davis for their R.B. Miller and Dissertation Awards. The authors also thank the National Cancer Institute (U19CA113298), the National Institute for General Medical Sciences (RO1-GM076151), and the National Science Foundation (NMR spectrometers; CHE-0443516 and CHE-9808183). This work was in part performed under the auspices of the United States Department of Energy by Lawrence Livermore National Laboratory under contract number DE-AC52-07NA27344.

Supporting Information Available: Analytical data for all new compounds and bioassay data for **3–11**. This material is available free of charge via the Internet at <http://pubs.acs.org>.

References

- (1) Lin, K. C.; Castro, A. C. Very late antigen 4 (VLA4) antagonists as anti-inflammatory agents. *Curr. Opin. Chem. Biol.* **1998**, *2*, 453–457.
- (2) Yusut-Makagiansar, H.; Anderson, M. E.; Yakovleva, T. V.; Murray, J. S.; Siahaan, T. J. Inhibition of LFA-1/ICAM-1 and VLA-4/VCAM-1 as a therapeutic approach to inflammation and autoimmune diseases. *Med Res. Rev.* **2002**, *22*, 146–167.
- (3) Holzman, B.; Gossler, U.; Bittner, M. α_4 integrins and tumor metastasis. *Curr. Top. Microbiol. Immunol.*, **1998**, *231*, 125–141.
- (4) Vincent, A. M.; Cawley, J. C.; Burthem, J. Integrin function in chronic lymphocytic leukemia. *Blood* **1996**, *87*, 4780–4788.
- (5) Marco, R. A.; Diaz-Montero, C. M.; Wygant, J. N.; Kleinerman, E. S.; McIntyre, B. W. α_4 integrin increases anoikis of human osteosarcoma cells. *J. Cell. Biochem.* **2003**, *88*, 1038–1047.
- (6) Peng, L.; Liu, R.; Marik, J.; Wang, X.; Takada, Y.; Lam, K. S. Combinatorial chemistry identifies high-affinity peptidomimetics against $\alpha_4\beta_1$ integrin for in vivo tumor imaging. *Nat. Chem. Biol.* **2006**, *2*, 381–387.
- (7) Carpenter, R. D.; Andrei, M.; Lau, E. Y.; Lightstone, F. C.; Liu, R.; Lam, K. S.; Kurth, M. J. Highly potent, water soluble benzimidazole antagonist for activated $\alpha_4\beta_1$ integrin. *J. Med. Chem.* **2007**, *50*, 5863–5867.
- (8) Perkins, J. J.; Zartman, A. E.; Meissner, R. S. Synthesis of 2-(alkylamino)benzimidazoles. *Tetrahedron Lett.* **1999**, *40*, 1103–1106.
- (9) Oh, Y.-H.; Han, H.-K. Pharmacokinetic interaction of tetracycline with nonsteroidal anti-inflammatory drugs via organic anion transporters in rats. *Pharm. Res.* **2005**, *53*, 75–79.
- (10) Babu, E.; Takeda, M.; Shinichi, N.; Yasuna, K.; Toshinori, Y.; Ho, C. S.; Takashi, S.; Dhanapal, S.; Hitoshi, E. Human organic anion transporters mediate the transport of tetracycline. *Jpn. J. Pharmacol.* **2002**, *88*, 69–76.
- (11) Carpenter, R. D.; DeBerdt, P. B.; Lam, K. S.; Kurth, M. J. A carbodiimide-based library method. *J. Comb. Chem.* **2006**, *8*, 907–914.
- (12) Carpenter, R. D.; Lam, K. S.; Kurth, M. J. Microwave-mediated heterocyclization to benzimidazo[2,1-*b*]quinazolin-12(5*H*)-ones. *J. Org. Chem.* **2007**, *72*, 284–287.
- (13) Grazioli, A.; Alves, C. S.; Konstantopoulos, K.; Yang, J. T. Defective blood vessel development and pericyte/pvSMC distribution in α_4 integrin-deficient mouse embryos. *Dev. Biol.* **2006**, *293*, 165–177.
- (14) Kaiser, E.; Colescott, R. L.; Bossinger, C. D.; Cook, P. I. Color test for detection of free terminal amino groups in the solid-phase synthesis of peptides. *Anal. Biochem.* **1970**, *34*, 595–598.
- (15) Sayigh, A. A. R.; Ulrich, H.; Potts, J. S. Reaction of arylamines with diethylthiocarbonyl chloride. New synthesis of aryl isothiocyanates. *J. Org. Chem.* **1965**, *30*, 2465–2466.
- (16) Bowne, D. W.; Dyson, G. W. *J. Chem. Soc.* **1935**, 178.
- (17) Jakobsen, C. M.; Denmeade, S. R.; Isaacs, J. T.; Gady, A.; Olsen, C. E.; Christensen, S. B. Design, synthesis, and pharmacological evaluation of thapsigargin analogues for targeting apoptosis to prostatic cancer cells. *J. Med. Chem.* **2001**, *44*, 4696–4703.
- (18) Budesinsky, M.; Exner, O. Correlation of carbon-13 substituent-induced chemical shifts: *meta*- and *para*-substituted methyl benzoates. *Magn. Reson. Chem.* **1989**, *27*, 585–591.
- (19) Sawhney, S. N.; Arora, S. K.; Singh, J. V.; Bansal, O. P.; Singh, S. P. Synthesis and anti-inflammatory activity of 2-amino- and 2-alkylamino-6-benzothiazoleacetic acids, 4-(2'-benzothiazolylamino)-4-(4'-substituted-2-thiazolyl-amino)- and 4-(4'-substituted-3'-alkyl-4'-thiazoline-2'-imino)phenylacetic acids. *Indian J. Chem., Sect. B: Org. Chem. Incl. Med. Chem.* **1978**, *16*, 605–609.
- (20) Nakayama, A.; Machinaga, N.; Yoneda, Y.; Sugimoto, Y.; Chiba, J.; Watanabe, T.; Imura, S. VLA-4 inhibitor. Patent JP11641, 2002.
- (21) Varma, R. Synthesis of substituted 2-anilinobenzoxazoles. *Curr. Sci.* **1976**, *45*, 53–54.
- (22) Tsubuki, T.; Nomura, M.; Sawada, T.; Kono, Y.; Sakoe, Y. Patent 258842, *Jpn. Kokai Tokkyo Koho*, **2000**.
- (23) Lusinskas, F.; Lawler, J. Integrins as dynamic regulators of vascular function. *FASEB J.* **1994**, *8*, 929–938.

JM800313F